Nuclear Inst. and Methods in Physics Research, A 902 (2018) 173–183

Contents lists available at ScienceDirect

Nuclear Inst. and Methods in Physics Research, A

journal homepage: www.elsevier.com/locate/nima

Scattered neutron background in thermal neutron detectors

E. Dian [a,b,c,*], K. Kanaki [b], G. Ehlers [d], R.J. Hall-Wilton [b,e], A. Khaplanov [b], T. Kittelmann [b], P. Zagyvai [a,c]

[a] Hungarian Academy of Sciences, Centre for Energy Research, 1525 Budapest 114., P.O. Box 49., Hungary
[b] European Spallation Source ESS ERIC, P.O Box 176, SE-221 00 Lund, Sweden
[c] Budapest University of Technology and Economics, Institute of Nuclear Techniques, 1111 Budapest, Műegyetem rakpart 9., Hungary
[d] Oak Ridge National Lab, Neutron Technologies Division, Oak Ridge, TN 37831-6475, USA
[e] Mid-Sweden University, SE-851 70 Sundsvall, Sweden

ARTICLE INFO

Keywords:
ESS
Neutron detector
Neutron scattering
Monte Carlo simulation
Geant4
Validation

ABSTRACT

Inelastic neutron scattering instruments require very low background; therefore the proper shielding for suppressing the scattered neutron background, both from elastic and inelastic scattering is essential. The detailed understanding of the background scattering sources is required for effective suppression. The Multi-Grid thermal neutron detector is an Ar/CO_2 gas filled detector with a $^{10}B_4C$ neutron converter coated on aluminium substrates. It is a large-area detector design that will equip inelastic neutron spectrometers at the European Spallation Source (ESS). To this end a parameterised Geant4 model is built for the Multi-Grid detector. This is the first time thermal neutron scattering background sources have been modelled in a detailed simulation of detector response. The model is validated via comparison with measured data of prototypes installed on the IN6 instrument at ILL and on the CNCS instrument at SNS. The effect of scattering originating in detector components is smaller than effects originating elsewhere.

1. Introduction

Inelastic neutron scattering is a very powerful technique for exploring atomic and molecular motion, as well as magnetic and crystal field excitations [1]. Time-of-Flight (ToF) spectrometers allow a broad phase space to be measured in a single setting; this is typically achieved with a large area detector array [2]. In typical state-of-the-art neutron instruments [2–8], this detector array can be 10–50 m^2. One of the main performance criteria of these spectrometers is typically defined by the Signal-to-Background Ratio (SBR), therefore understanding and enhancing the latter is important for the instrument optimisation. In particular, scattered neutrons have a significant contribution to the SBR. The estimation of the SBR is done currently on a series of prescriptions based on observations of historical instrument installation.

As a consequence of the recent restructuring of the ^{3}He market [9], a need for cost effective ^{3}He-replacing detector solutions is raised [10], especially for inelastic neutron scattering instruments, where large area detectors with high SBR are required. A potent new solution for this type of instruments is the Multi-Grid detector [11,12], which will be used for the three Time-of-Flight chopper spectrometers at ESS [13–16]. The Multi-Grid design was invented at the Institut Laue-Langevin (ILL) [17,18], and the detector now is jointly developed by the ILL and the ESS within the CRISP [19] and BrightnESS [20] projects.

The Multi-Grid detector is an Ar/CO_2-filled proportional chamber with a solid boron-carbide ($^{10}B_4C$) neutron converter, enriched in ^{10}B [21–23]. The basic unit of the Multi-Grid detector is the grid, an aluminium frame; thin aluminium lamellas, coated on their both sides with boron-carbide, the so called blades are placed in this frame, parallel with each other and the entrance window of the grid, dividing the grid into cells. In the detector the grids are structured into columns, and this way the cells one above the other form tubes, and the signals are readout both from the frames and the anode wires that go through the whole length of the column in the centre of the cells. The planned detector modules and the prototypes are built of these columns. A series of small size prototypes and large scale demonstrators are already built and tested at different sources and instruments [24,25], and the development of the detector has already entered the up-scaling phase. As Multi-Grid is a large area detector, full scale design is limited by cost considerations. However, detailed Monte Carlo modelling can help tackle the limitations and provide guidelines for the up-scaling design, which is particularly important for detectors that have to provide excellent SBR $\sim \mathcal{O}(10^5)$.

* Corresponding author at: Hungarian Academy of Sciences, Centre for Energy Research, 1525 Budapest 114., P.O. Box 49., Hungary.
E-mail address: dian.eszter@energia.mta.hu (E. Dian).

https://doi.org/10.1016/j.nima.2018.04.055
Received 18 January 2018; Received in revised form 13 April 2018; Accepted 25 April 2018
Available online 3 May 2018

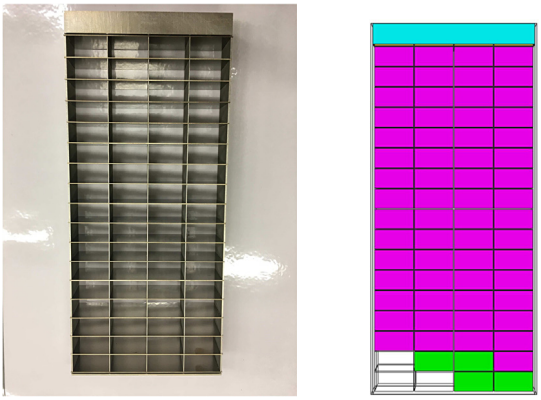

(a) (b)

Fig. 1. Real grid 1(a) and grid geometry implemented in Geant4 1(b).

The two-fold aim of the current study is to introduce a detailed Geant4 model of the Multi-Grid detector including validation against datasets of experiments [24,25] performed on existing demonstrators, as well as to identify the various components of the scattered neutron background, induced by cold and thermal neutrons internally and externally to the Multi-Grid detector.

The Geant4 model of the Multi-Grid detector is presented in Section 2. In Section 3, the model validation against the measured ToF flight distance and energy transfer data from the IN6 (Cold neutron time-focusing time-of-flight spectrometer IN6-Sharp), and in Sections 4.1 and 4.2 the CNCS (Cold Neutron Chopper Spectrometer) demonstrator tests are shown. As part of the reproduction of the CNCS demonstrator measured data, a study of the individual contributions to the scattered neutron background is also discussed. In Section 4.3 results regarding the neutron scattering on the aluminium components of the detector vessel of the CNCS detector are described. Finally, in Section 5 the obtained results are concluded from the aspects of validation, and the further utilisation of the built model for detailed background analysis and for the optimisation of the detector vessel design is also shown.

2. Geant4 model of multi-grid detector

A general, parameterised Geant4 [26–28] model of the Multi-Grid detector has been developed within the ESS Detector Group Simulation Framework [29], with the usage of the NXSG4 [30] extension library. The latter enables the crystalline structure of aluminium, used in the detector frame. For all other components, standard Geant4 materials are used. The physics list is the standard QGSP_BIC_HP, except when polyethylene is included in the materials, in which case a customised physics list is preferred instead [31], due to the relevance of thermal scattering on the high hydrogen-content of the polyethylene.

From the flexible, full-scale model, the realistic models of two demonstrators that were tested at the IN6 [24] at ILL and at the CNCS [25] at SNS were also prepared. To reach a very flexible geometry, a few simplifications were done. The basic unit of the model is the so called cell, a $2 \times 2 \times 1$ cm^3 counting gas volume of the detector, delimited by B_4C-coated aluminium blades. Therefore everything has to be symmetrical at the cell level, like the blade thicknesses, the cell volumes and most importantly the coating thicknesses. This estimation is applied in the basic model and the IN6, but in the CNCS demonstrator a series of different coating thicknesses are used (13×0.5 μm$+14\times1.0$ μm$+6\times1.5$ μm$+1\times1.0$ μm). So for the latter model, the coating thicknesses are hard-coded to fit the real prototype, and so the grid became the basic unit for this detector. The anode wires and the electronics of the detector are excluded from the models, as it is shown in Fig. 1. The major parameters of the prepared models are shown in Table 1.

The simulated primary neutrons are generated at the sample position. The sample is placed at the centre of the geometry, with the z direction chosen as the beam direction, leading to x as horizontal and to y as vertical coordinates. The sample-to-detector distance is defined as the shortest distance from the sample position to the entrance window of the detector: grid window or vessel window, in case the latter is enabled. Basic particle guns, like a pencil beam, 4π and cylindrical sources are used, as well as targeted beams to irradiate only the detector surface. Although the physics of the samples themselves is not implemented in the simulations, the above listed particle guns are defined both as point and volume sources (1 x 1 x 1 cm^3 cube or cylinder with 1 cm diameter). Some instrument effects are introduced via the source definition, like the energy distribution of the incident primary neutrons.

In chopper spectroscopy the data of interest are the momentum- and energy transfer of the scattered neutrons. These are derived from the primary measured quantities: the detection coordinates (giving the flight distance) and the ToF. The flight distance is defined as the distance from the sample position to the detection coordinates. The simulated detection coordinates are reduced to the centre of the cell in which the neutron is detected, despite the higher resolution of the simulation. ToF is simulated from sample position. The detector model is validated against these raw measured quantities of the IN6 demonstrator, and a detailed study of scattered neutron background is also performed regarding the energy transfer in the CNCS demonstrator.

3. Model of demonstrator test on the IN6 instrument at ILL

At the IN6 experiment the demonstrator (Fig. 2(a)) is tested with neutron beams of 4.1, 4.6 and 5.1 Å (i.e. 4.87, 3.87 and 3.15 meV, respectively), irradiating the entire entrance surface. The same geometry is implemented in the simulation (Fig. 2(b)) and validated against the measured and published ToF spectra. Due to the lack of data on the measurement setup (e.g., exact chopper settings and timing references), the measured and simulated ToF spectra are compared either in a relative time scale, or all of them are scaled to the time scale of the simulation, in which the neutrons and their respective ToF are generated at the sample position.

The detector geometry is irradiated with pencil and targeted beams, in order to illuminate the entrance surface (see Fig. 3), both with sharply mono-energetic and Gauss-smeared initial neutron energy distributions of 4.1, 4.6 and 5.1 Å. For preparing the demonstrative study on the 2-dimensional distributions of the ToF spectra as the function of the depth of detection, a minor simplification was performed: for this demonstration only 1 column of the detector model was used, since in this case z-coordinate one-to-one corresponds to the detection depth in detector, leading to an easy readout.

3.1. Simulation results for IN6 Demonstrator detector

For the IN6 experiment, ToF spectra and 2D detection depth dependent ToF spectra are simulated and compared to the published measurements at 4.1, 4.6 and 5.1 Å wavelengths. In Fig. 4 the comparison of the measured (Figs. 4(a)–4(c)) and the simulated ToF-spectra as a function of the depth of detection is presented with mono-energetic (Figs. 4(d)–4(f)) and Gaussian (Figs. 4(g)–4(i)) incident neutron energy distributions. At all wavelengths the main path of the incident detected neutrons clearly appears as a skew line both in the measured and the simulated distributions. The angle of the path is related to the neutron's velocity.

Beside the main path, at 4.1 and 4.6 Å wavelengths that are below the aluminium Bragg edge [32,33], the traces of the detected scattered neutrons appear as well. On the one hand, in the near surface region a triangle-shaped shadow appears beside the main neutron path, produced by the neutrons detected after scattering on the intermediate aluminium blades. On the other hand, a short, opposite direction skew line appears